Spectroscopic analysis of the 1:1 tetracyanoquinodimethane-9,9'-bifluorenylidene charge-transfer complex: Infrared, UV-visible and resonance Raman spectra

2 AUTHORS, INCLUDING:

Leonardo Angeloni
University of Florence
47 PUBLICATIONS **666** CITATIONS

Spectroscopic Analysis of the 1:1 Tetracyanoquinodimethane–9,9'-Bifluorenylidene Charge-Transfer Complex: Infrared, UV–Visible and Resonance Raman Spectra†

L. Angeloni*
Istituto di Chimica Fisica, Università di Firenze, via Gino Capponi 9, Firenze, Italy

G. Sbrana
Centro di Studio sulla Chimica e la Struttura dei Composti Eterociclici del CNR, Istituto di Chimica Organica, Università di Firenze, via Gino Capponi 9, Firenze, Italy

The 1:1 TCNQ–9,9'-bifluorenylidene π-complex (TCNQ = tetracyanoquinodimethane) was investigated by infrared, UV–visible and Raman spectroscopy. Resonance Raman spectra of the solid were measured and from the analysis of the excitation profiles the lower energy electronic levels of TCNQ and 9,9'-bifluorenylidene in the complex were identified. A blue shift of the low-lying electronic levels of the interacting molecules was observed. The mechanisms responsible for the Raman intensity of TCNQ in the complex and in solution are discussed.

INTRODUCTION

Tetracyanoquinodimethane (TCNQ) is a strong electron acceptor and is known to form in the solid state a variety of complexes ranging from highly conducting charge-transfer complexes[1-3] to almost non-conducting π-complexes. The spectroscopic properties of these materials are of enormous interest but the results reported so far are not extensive, particularly for the highly conducting charge-transfer compounds. This is mainly due to their peculiar optical properties. The infrared spectra of charge-transfer complexes are characterized by a broad and unresolved electronic band extending from the UV to the far-infrared region superimposed on the purely vibrational peaks. The high metallic reflectivity of the crystals, which appear shiny and black, makes the measurement of the Raman spectra a formidable task. More extensive results have been obtained in the case of the π-complexes of TCNQ with highly symmetric organic molecules such as pyrene,[4] coronene[5] and perylene.[6] The characterization of these compounds may turn out to be very useful for the study of the electronic properties of the semiconducting complexes of TCNQ whenever direct spectroscopic information on the latter is not available.

In this paper we discuss the spectroscopic features of a 1:1 complex of TCNQ with 9,9'-bifluorenylidene (Biflu) which we have recently synthesized[7] (Fig. 1). Infrared, electronic and Raman spectra were measured and compared with those of the Biflu[8] and TCNQ[9-11] non-complexed molecules.

Slight differences appear in the electronic and Raman spectra of the complex, revealing that a strong interaction occurs between Biflu and TCNQ in π-complex formation. Accordingly, we also recorded the resonance Raman spectra and measured the exciting frequency dependence of the Raman intensities to obtain the excitation profiles for some typical bands of the complex. This type of analysis provided information on the low-lying electronic levels of the parent molecules, which are particularly affected by complexation.

EXPERIMENTAL

The complex was prepared by mixing equimolar solutions in acetonitrile of TCNQ and Biflu. After several hours, black shining crystals were obtained from the mixture. The precipitate was filtered and washed several times with diethyl ether. [Elemental analysis: calculated for $C_{18}H_{20}N_4$, C 85.70, H 3.76, N 10.53; found, C 85.63, H 3.85, N 10.52%.] The temperature, time of heating and proportions of the reagents did not affect the stoichiometry of the compound. The resistivity of
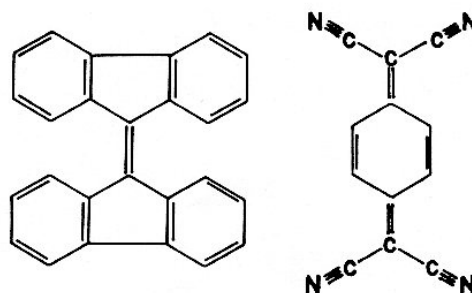
Figure 1. 9,9'-Bifluorenylidene and TCNQ molecules.

the complex was measured on powder pressed at ca 5 ton cm^{-2} using the 'four probes' method[12] in order to eliminate the contact resistance. The average value was found to be $\rho = 1500\,\Omega$ cm. Biflu was prepared and purified according to the procedure reported in Ref. 13. Pure TCNQ was obtained by several crystallizations of the commercial product (Fluka) from acetonitrile.

The infrared spectra in nujol mull and KBr pellets were measured with a Perkin–Elmer 225 spectrophotometer. The pellets were pressed under a pressure of less than 5 ton cm^{-2} at room temperature. Changes in the infrared spectra were observed using pellets previously heated or prepared under higher pressures. Electronic absorption spectra of the complex and of the pure TCNQ and Biflu in NaCl pellets were obtained in the 900–230 nm region using a Cary 14 spectrophotometer.

The resonance Raman spectra were registered using a Jobin–Yvon HG 2S monochromator, a cooled RCA-C 31034A photomultiplier and a photon counting system. An argon ion laser selecting the 457.9, 476.5, 488.0, 496.5, 501.7 and 514.5 nm exciting lines was employed to obtain spectra on samples finely dispersed in KBr powder and containing a small amount of NaNO$_3$. Intensity measurements of the Raman bands were made using the band at 1068 cm^{-1} of NaNO$_3$ as internal standard. The average experimental error was estimated to be less than 15%. A rotating cell device was employed to avoid thermal decomposition.

RESULTS AND DISCUSSION

Infrared spectra

The infrared spectrum of the complex in KBr pellet is shown in Fig. 2. The corresponding frequencies are listed in Table 1 and compared with those of solid Biflu and TCNQ. The broad absorption band which is characteristic of the semiconducting complexes[15,16] has not been observed. From Table 1, it can be seen that the bands of the two components are slightly shifted in frequency in the complex, with only minor changes in the intensity pattern. Some differences occur only in the 900–800 cm^{-1} region where the spectrum of the

complex shows fewer bands than those expected from Biflu and TCNQ. Actually, only four bands are present, at 871, 860, 837 and 804 cm^{-1}, in the spectrum of the complex in comparison with the three bands of the TCNQ at 878, 863 and 811 cm^{-1}. The band at 837 cm^{-1}, which has no clear counterpart in the spectra of the components, must be correlated with the 863 cm^{-1} mode of TCNQ on the basis of its intensity. This mode can be identified as an out-of-plane bending motion and, because of its sensitivity to the π-electron interaction, can be taken as diagnostic of the formation of the complex. A similar behaviour was also observed in the 3:1 and 1:1 TCNQ–coronene complexes for the out-of-plane bending modes.[5]

It should be noted that the multiplicity of the infrared bands of each component remains unchanged in the complex and no evidence exists of the activation of the Raman modes. This means that the interacting molecules retain their proper symmetry or at least the centre of inversion.

Electronic spectra

UV–visible spectra of solid Biflu, TCNQ and π-complex are shown in Fig. 3. The spectrum of TCNQ consists of a broad band showing a fine structure with vibronic peaks at 444, 408, 375 and 340 nm. The pattern is similar to that observed in the vapour and solution spectra[11] but the separation of the vibronic peaks in the solid is different. In the latter, the average spacing among the vibronic components ($\sim$1900 cm^{-1}) suggests a large contribution of the symmetric CN stretching mode at 2225 cm^{-1}. In the vapour and in solution, a lower frequency mode seems to be responsible for the observed vibrational progression.

The spectrum of TCNQ differs substantially from those of the π-complex and of the Biflu, which show a broad structureless band with only two maxima, at 440, 500 and 466, 520 nm, respectively. These spectra have similar patterns except in the lower wavelength region where two additional bands appear in the spectrum of the complex, at 630 and 830 cm^{-1}. These bands are characteristic of all charge-transfer complexes[4,5] and can be reasonably attributed to charge-transfer transitions from the Biflu to the TCNQ molecules.
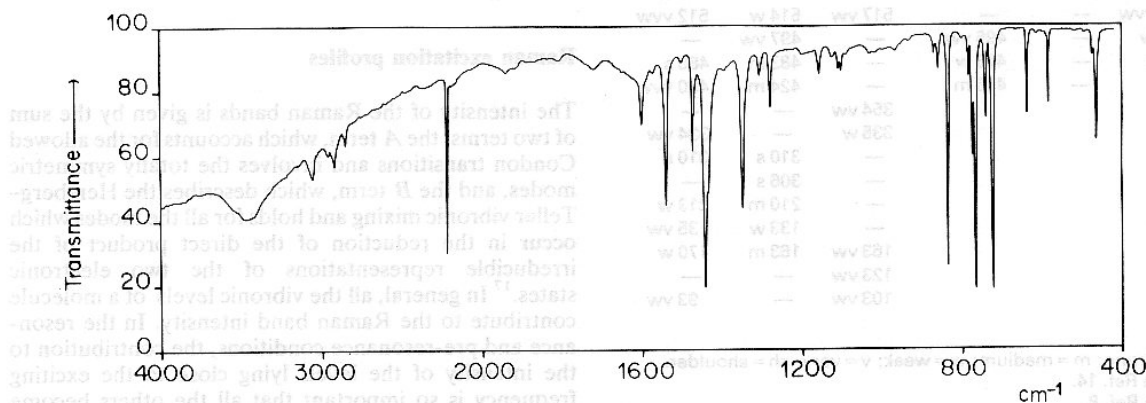
Figure 2. Infrared spectrum of solid 1:1 TCNQ–Biflu complex.

Table 1. Vibrational frequencies (cm⁻¹) of solid TCNQ, Biflu and the 1:1 complex

Infrared[a]			Raman[a]		
TCNQ[b]	Biflu[c]	Complex	TCNQ[b]	Biflu[c]	Complex
2218 s	—	2219 s	2225 m	—	2220 w
—	1604 w	1602 w	—	1635 m	1640 vw
—	1573 vw	1575 vw	—	1620 w	—
1541 s	—	1541 m	1600 w	—	1606 w
—	1476 m	1475 m	—	1595 w	—
—	1470 sh	1470 sh	—	1550 vs	1546 vs
—	1450 m	—	—	1527 w	1528 w
—	1443 s	1443 s	—	1499 vvw	1502 vvw
—	1438 sh	1438 sh	—	—	1478 vvw
1365 w	—	—	—	1469 vvw	1462 w
1352 m	1349 m	1349 m	1454 s	—	1456 w
—	1339 vvw	1339 sh	—	1448 vw	—
—	1310 vvw	1310 w	—	1435 m	1439 w
1284 vvw	1281 w	1280 w	1398 vvw	—	1390 vw
1205 vvw	—	1200 vvw	—	1359 vw	1364 w
1155 vvw	1150 vvw	1155 w	1310 vvw	1309 w	—
1135 w	—	—	1234 vvw	1230 m	1231 m
1124 w	—	1127 w	—	1219 s	1221 m
1110 w	1110 w	1111 w	1206 m	—	1204 vw
—	1100 w	1102 w	—	1195 m	—
1090 w	—	1090 w	1189 vw	—	—
1046 w	—	—	—	1162 vw	—
—	1034 w	1034 w	—	1134 w	1141 w
976 w	—	—	—	1109 w	1120 w
961 w	—	963 vvw	—	1091 w	—
—	938 vvw	934 vvw	—	1071 w	1072 vw
—	953 vvw	955 vvw	1064 vvw	—	—
878 w	—	—	—	1031 m	1032 w
—	871 w	871 w	—	1031 m	1032 w
—	860 vvw	860 vvw	—	1011 vvw	—
—	842 vvw	—	1003 vvw	—	—
863 s	—	837 s	964 vvw	952 vvw	942 vvw
811 w	—	804 vvw	—	882 w	890 w
—	785 m	784 w	—	845 vw	—
772 w	—	776 w	816 w	—	818 vw
—	761 s	767 s	—	785 m	783 w
750 vvw	—	—	—	761 w	766 vw
—	741 vvw	741 m	754 w	752 m	756 vw
—	718 s	721 s	—	—	730 w
—	637 m	639 m	718 w	—	—
623 m	—	—	—	699 w	—
—	612 m	612 vw	—	658 w	—
598 w	—	—	638 vvw	—	645 vvw
—	582 m	584 m	596 w	—	612 vw
548 vvw	—	—	—	566 m	568 w
512 vvw	—	—	517 vvw	514 w	512 vvw
498 w	—	495 vvw	—	497 vvw	—
475 s	—	475 w	—	483 m	485 s
—	—	465 m	—	424 m	430 vvw
			354 vvw	—	—
			335 w	—	334 vvw
			—	310 s	310 s
			—	306 s	—
			—	210 m	213 w
			—	133 w	135 vvw
			163 vvw	163 m	170 w
			123 vvw	—	—
			103 vvw	—	93 vvw

[a] s = strong; m = medium; w = weak; v = very; sh = shoulder.
[b] From Ref. 14.
[c] From Ref. 8.
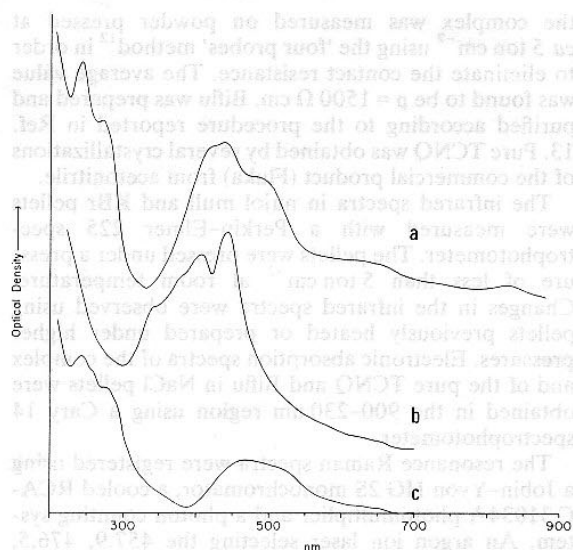
Figure 3. Electronic spectra of solid: (a) 1:1 TCNQ–Biflu complex; (b) TCNQ; (c) Biflu.

Resonance Raman spectra

The resonance Raman spectra of the π-complex were recorded with six wavelengths of the argon ion laser. For the sake of simplicity, only Raman spectra recorded with three wavelengths, viz. 457.9, 488.0 and 514.5 nm, are shown in Fig. 4. Observed frequencies are listed in Table 1 together with those of solid Biflu and TCNQ. In the spectrum of the complex the band at 1068 cm⁻¹ is due to the $NaNO_3$ and was chosen as internal standard for intensity measurements. Large intensity changes are observed in the Raman spectrum. These depend on the exciting frequency and involve mainly the totally symmetric modes of the two components. Bands which correspond to Biflu modes are enhanced and those relative to TCNQ vibrations decrease by lowering the frequency of the exciting line.

As for the infrared results no significant changes of the Biflu and TCNQ frequencies are observed in the Raman spectrum. This confirms that not only is the molecular symmetry conserved, the force constants of the interacting molecules remain practically unchanged.

Raman excitation profiles

The intensity of the Raman bands is given by the sum of two terms: the A term, which accounts for the allowed Condon transitions and involves the totally symmetric modes, and the B term, which describes the Herzberg–Teller vibronic mixing and holds for all the modes which occur in the reduction of the direct product of the irreducible representations of the two electronic states.[17] In general, all the vibronic levels of a molecule contribute to the Raman band intensity. In the resonance and pre-resonance conditions, the contribution to the intensity of the levels lying close to the exciting frequency is so important that all the others become negligible. The analysis of the excitation profiles gives
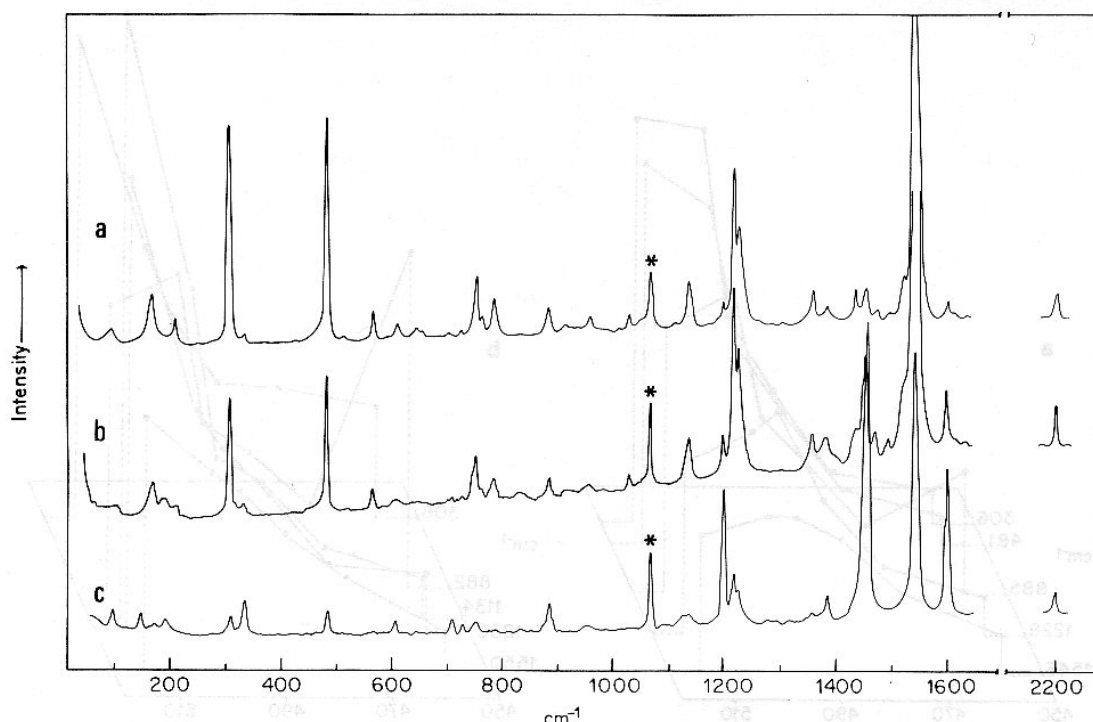
Figure 4. Resonance Raman spectra of solid 1:1 TCNQ-Biflu complex registered with the (a) 514.5 nm, (b) 488.0 nm and (c) 457.9 nm exciting lines. The asterisks identify the band of $NaNO_3$ at 1068 cm^{-1} used as reference.

evidence for those vibronic states which are mainly responsible for the enhancement process of the Raman bands.

It has been shown that the A term is the most important under resonance, i.e. when the frequency of the exciting radiation falls in the electronic absorption band. In the Born–Oppenheimer approximation, by following the Herzberg–Teller expansion for adiabatic functions, the elements of the polarizability tensor $A_{(\rho\sigma)}$ responsible for the Raman intensity are given by

$$A_{(\rho\sigma)01} = \sum_{ev} \frac{(M_\rho)_{g^0e^0}(M_\sigma)_{g^0e^0}\langle 0|v\rangle\langle v|1\rangle}{((E_{g^0e^0}+\varepsilon_v-E_l)-i\Gamma_{ev})}$$

where $(M_\rho)_{g^0e^0}$ is a component of the transition moment connecting the pure electronic ground (g^0) and excited (e^0) states, $\langle 0|v\rangle$ and $\langle v|1\rangle$ are the vibrational overlap integrals, $E_{g^0e^0}$ is the energy difference between the electronic states, ε_v the vibrational energy in the excited state, E_l the energy associated with the excitation frequency and Γ_{ev} the homogeneous damping factor.

The above expression shows that the excitation profiles, i.e. the dependence of the Raman band intensity on the frequency of the exciting line, is governed mainly by two factors: the frequency factor, which causes strong enhancements at resonance, and the damping factor, which gives rise to band broadening and then to smooth profiles. Therefore, even if the cross-sections are generally larger in resonance, the strongest intensity changes occur in pre-resonance where the damping factor is less important. The slope of the excitation profiles, which is a function of the difference between the vibronic and the exciting

frequencies, can be qualitatively correlated with the energy shift of the vibronic levels from which the corresponding Raman bands borrow their intensity.

The excitation profiles shown in Figs 5 and 6 were drawn on the basis of intensity measurements related to an internal standard and normalized to the values observed in the Raman spectrum recorded with 488.0 nm radiation. These curves describe the behaviour of the most significant Raman bands of Biflu and TCNQ molecules in the pure crystals (b) and in the π-complex (a).
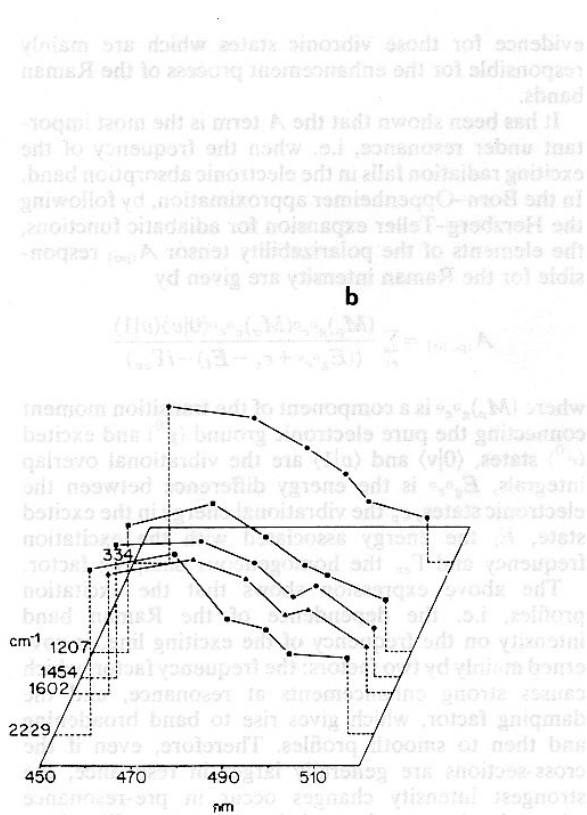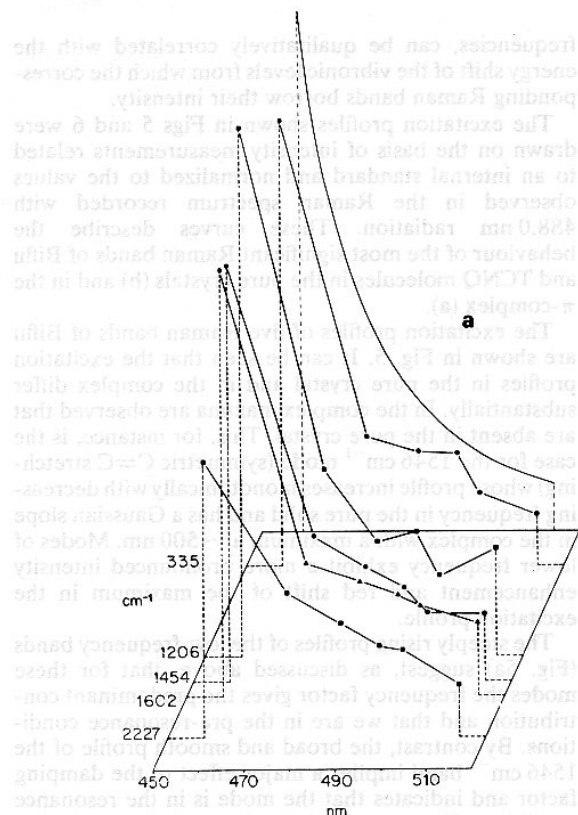
The excitation profiles of five Raman bands of Biflu are shown in Fig. 5. It can be seen that the excitation profiles in the pure crystal and in the complex differ substantially. In the complex maxima are observed that are absent in the pure crystal. This, for instance, is the case for the 1546 cm^{-1} mode (symmetric C=C stretching) whose profile increases monotonically with decreasing frequency in the pure solid and has a Gaussian slope in the complex with a maximum at ~500 nm. Modes of lower frequency exhibit a more pronounced intensity enhancement and red shift of the maximum in the excitation profile.

The steeply rising profiles of the low-frequency bands (Fig. 5a) suggest, as discussed above, that for these modes the frequency factor gives the predominant contribution and that we are in the pre-resonance conditions. By contrast, the broad and smooth profile of the 1546 cm^{-1} band implies a major effect of the damping factor and indicates that the mode is in the resonance condition. The general behaviour of the excitation profiles and the dependence of the maxima on the mode frequency strongly suggest that 0–1 transitions are
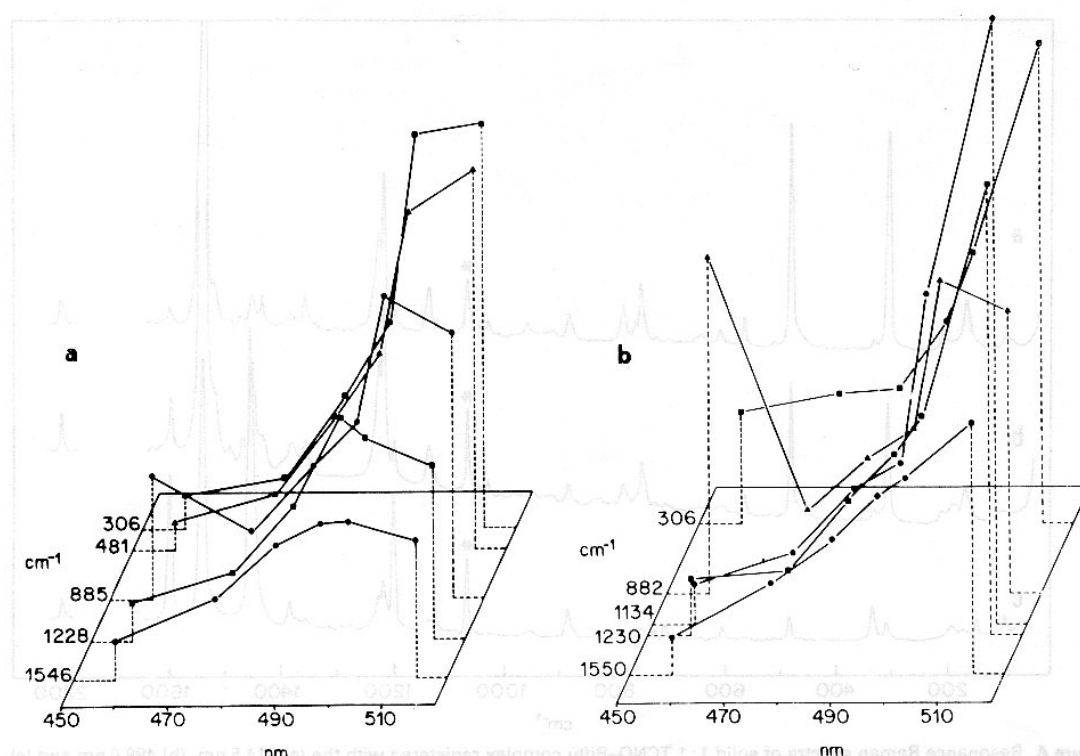
Figure 5. Excitation profiles of some Raman bands of (a) complexed and (b) pure Biflu obtained using six different frequencies of the Ar ion laser (see text).

Figure 6. Excitation profiles of some Raman bands of (a) complexed and (b) pure TCNQ obtained using six different frequencies of the Ar ion laser (see text). The smooth curve is calculated using the F_A^2 frequency factor with $\lambda_{max.} = 404$ nm ($\nu_e = 24752$ cm^{-1}).

responsible for the shape of the electronic absorption band. According to this, the transition corresponding to the $1546 \, cm^{-1}$ mode can be located at $\sim 500 \, nm$.

Similar conclusions were also reached in the case of Biflu in solution[8] where band enhancement was found to depend on the 0–1 term of the vibrational progression of the lower electronic state.

The plots in Fig. 6 refer to the TCNQ molecule and describe the frequency dependence of five bands from the exciting line in the pure solid (Fig. 6b) and in the complex (Fig. 6a). In this case the curves exhibit a pattern opposite to that of Biflu, increasing in going towards the shorter wavelength region. In the complex, each band is affected differently by changing the frequency of the exciting radiation and band enhancements are always observed (5–10 times) in going from 514.5 to 457.9 nm excitation. The largest enhancement occurs for the $1206 \, cm^{-1}$ band and the smallest for the $2227 \, cm^{-1}$ mode.

In Fig. 6a we also report the excitation profile calculated according to the F_A^2 frequency factor of the Albrecht theory[17] with $\lambda_{max} = 404 \, nm$ (smooth line). This curve fits very well those for the 1206 and $335 \, cm^{-1}$ bands. This agreement implies a negligible contribution of the damping factor and therefore the occurrence of pre-resonance conditions.

In the pure solid, all the bands show small intensity changes and their profiles exhibit a maximum at $\sim 475 \, nm$. The interpretation of the observed profiles is difficult at present. It can be noted that also in solution a slight dependence of the intensity on the exciting frequency has been found[18] and some bands (1602, $1454 \, cm^{-1}$) appear to depend on the B term and some others (2227, $1206 \, cm^{-1}$) on both A and B terms.[17,18] The profiles occurring in solution could be explained in terms of different conformations of the molecule in the lowest excited electronic state as a consequence of interactions with the solvent. Such an explanation is not possible for the complex where a single molecular configuration of TCNQ is probably favoured by crystal field and interaction forces with the counter ion.

Also in the case of TCNQ, a blue shift of the lower electronic state occurs on complexation. From the excitation profiles, the lower electronic state can be tentatively located at $\sim 400 \, nm$. This compares reasonably with the experimental absorption maximum in solution at 395 nm.

Acknowledgements

REFERENCES

1. J. Tanaka, M. Tanaka, T. Kawai, T. Takaba and O. Maki, *Bull. Chem. Soc. Jpn.* **49**, 2358 (1976).
2. D. J. Sandman, *Mol. Cryst. Liq. Cryst.* **23**, 1235 (1967).
3. T. Kondow, K. Siratori and H. Inokuci, *J. Phys. Soc. Jpn.* **23**, 98 (1967).
4. K. D. Truong and A. D. Bandrauk, *Chem. Phys. Lett.* **44**, 1232 (1976).
5. K. D. Truong and A. D. Bandrauk, *Can. J. Chem.* **55**, 1712 (1977).
6. A. D. Bandrauk, K. D. Truong, V. R. Salares and H. J. Bernstein, *J. Raman Spectrosc.* **8**, 5 (1979).
7. G. Sbrana, L. Angeloni and S. Panerai, *J. Quantum Chem.* **19**, 1157 (1981).
8. L. Angeloni, G. Sbrana and S. Panerai, *J. Raman Spectrosc.* **12**, 30 (1982).
9. R. Bozio, A. Girlando and C. Pecile, *J. Chem. Soc., Faraday Trans. II* **71**, 1237 (1975).

10. A. Girlando and C. Pecile, *Spectrochim. Acta, Part A* **29**, 1859 (1973).
11. R. R. Pennelly and C. J. Eckardt, *Chem. Phys.* **12**, 86 (1976).
12. V. Walatka and J. H. Perlstein, *Mol. Cryst. Liq. Cryst.* **15**, 269 (1971).
13. G. P. De Gunst, *Recl. Trav. Chim. Pays. Bas* **88**, 801 (1969).
14. B. Lunelli and C. Pecile, *J. Chem. Phys.* **52**, 2375 (1970).
15. H. Poradowska, W. Czuba, K. Lorenze and A. Chyla, *Rec. J. Neth. Soc.* **96**, 42 (1977).
16. L. R. Melby, R. J. Harder, W. R. Hertler, W. Mahler, R. E. Benson and W. E. Mochel, *J. Am. Chem. Soc.* **84**, 1374 (1962).
17. A. C. Albrecht, *J. Chem. Phys.* **34**, 1476 (1961).
18. W. T. Wozniak, G. Depasquali and M. V. Klein, *Chem. Phys. Lett.* **40**, 93 (1976).